

# Tunable microwave pulse generation using discharge plasmas

Cite as: Appl. Phys. Lett. **109**, 124103 (2016); <https://doi.org/10.1063/1.4963268>

Submitted: 16 August 2016 . Accepted: 11 September 2016 . Published Online: 22 September 2016

David R. Biggs , and Mark A. Cappelli



View Online



Export Citation



CrossMark

## ARTICLES YOU MAY BE INTERESTED IN

### [A plasma photonic crystal bandgap device](#)

Applied Physics Letters **108**, 161101 (2016); <https://doi.org/10.1063/1.4946805>

### [A tunable microwave plasma photonic crystal filter](#)

Applied Physics Letters **107**, 171107 (2015); <https://doi.org/10.1063/1.4934886>

### [Waveguiding and bending modes in a plasma photonic crystal bandgap device](#)

AIP Advances **6**, 065015 (2016); <https://doi.org/10.1063/1.4954668>

Lock-in Amplifiers  
up to 600 MHz



Watch



## Tunable microwave pulse generation using discharge plasmas

David R. Biggs<sup>a)</sup> and Mark A. Cappelli

Mechanical Engineering Department, Stanford University, Stanford, California 94305, USA

(Received 16 August 2016; accepted 11 September 2016; published online 22 September 2016)

The response of a microwave resonant cavity with a plasma discharge tube inside is (continuously or intermittently) filled with a plasma and studied both numerically and experimentally. The resonance frequency of the cavity-plasma system is sensitive to plasma densities from  $10^{16}$  to  $10^{20} \text{ m}^{-3}$  corresponding to resonant frequencies of 12.3–18.3 GHz. The system is first characterized for its quasi-steady state response using a low frequency plasma discharge at 70 kHz and 125 V RMS. A plasma discharge is then driven with a high voltage pulse of 4 kV and a CW input microwave signal is converted to a pulsed output signal. The microwave pulse delay and pulse width are varied by selecting the input microwave frequency. The microwave input power is set to +20 dBm. The delay of the microwave pulse is also used as a diagnostic tool for measuring the variation of plasma density in time and, with numerical fitting, the discharge plasma recombination coefficient and diffusion timescales are estimated. *Published by AIP Publishing.*

[<http://dx.doi.org/10.1063/1.4963268>]

The use of plasmas as a means of tuning and tailoring electromagnetic devices is of interest for various applications such as high frequency communications and analog signal processing. One such device is the microwave resonant cavity, which has a resonance frequency dependent on the dielectric constant of the filling medium. Plasmas are tunable dielectric materials that may be used as the filling medium to control the frequency response of the cavity. Low-pressure plasmas must be employed at microwave frequencies of tens of gigahertz in order to avoid wave damping from excessive collisions. The drawback of low-pressure plasmas is that the timescales that govern ionization and recombination processes are long. Research in optimizing the plasma-microwave response time is needed in order to achieve fast tuning capabilities and high bandwidth in these devices.

Plasma-filled microwave cavities have historically been utilized as diagnostic tools for low pressure plasma discharges. Resonant methods require measuring the shift in the resonance frequency and the decrease in the quality factor of the plasma-filled cavity. Perturbation techniques are used to retrieve the electron number density and collision frequency.<sup>1–3</sup> Microwave resonant cavities with mercury discharge tubes co-axially centered along the cavity have also been studied using similar methods.<sup>4</sup> Perturbation techniques are limited to small number densities  $n_e \lesssim 0.1(\omega^2 m_e \epsilon_0 / e^2)$ , with  $n_e$  being the electron number density,  $\omega$  the measurement frequency,  $m_e$  and  $e$  the electron mass and charge, and  $\epsilon_0$  the permittivity of free space.<sup>5</sup> Theories have been developed in order to measure higher number densities without the assumption of small perturbations but are limited in applicability.<sup>6</sup> Other resonant methods use discharge tubes inserted transversely into rectangular waveguide cavities and make use of equivalent circuit parameters of lossy dielectric cylinders to extract the desired number density of the plasma to high values.<sup>7</sup> Microwave resonant methods have also found use in determining the total recombination rates in

pulsed plasmas by measuring the resonant frequency shift in time.<sup>8–10</sup>

Still, few microwave devices have incorporated plasmas for non-diagnostic use. Spark gaps have been used in rectangular waveguides as fast switches to reflect high power microwaves,<sup>11–13</sup> but reflect in broadband and are not tunable. More recently, plasma breakdown has been utilized as a power limiter in tunable cavity resonators<sup>14,15</sup> and low pressure discharge lamps have been used to tune photonic crystal cavities,<sup>16</sup> but both studies are in the quasi-steady state and do not explore the time dynamics of their systems.

In this work, we report on studies of the response of a microwave resonant cavity within a rectangular WR-62 waveguide to both continuous and pulsed discharge plasma. We explore the tuning capabilities both in the quasi-steady state and in time dynamical settings. The cavity acts as a band pass filter and transmits microwave signals at its resonant frequency. A discharge tube is placed transversely inside the cavity, parallel to the narrow waveguide walls, in order to introduce plasma either continuously or intermittently into the device.

The resonant cavity is designed and simulated with the commercial finite element electromagnetic software ANSYS HFSS 16. A quarter of the structure is reproduced in the three-dimensional simulations with electric and magnetic field symmetry boundary conditions accounting for the reduced geometry. Finite conductivity boundary conditions are set along the copper interfaces, and a quartz tube and a plasma cylinder are placed within the cavity and extend out beyond the cavity. The plasma is treated as a uniform lossy dielectric with a dielectric constant given by the Drude model

$$\epsilon_p = 1 - \frac{\omega_p^2}{\omega^2 - j\nu\omega} \quad \omega_p = \sqrt{\frac{n_e e^2}{\epsilon_0 m_e}} \quad (1)$$

Here,  $\omega_p$  is the plasma frequency and  $\nu$  is the total electron momentum transfer collision frequency. This is in accordance with the approach described by Wang and Cappelli.<sup>16</sup> The

<sup>a)</sup>buggs@stanford.edu

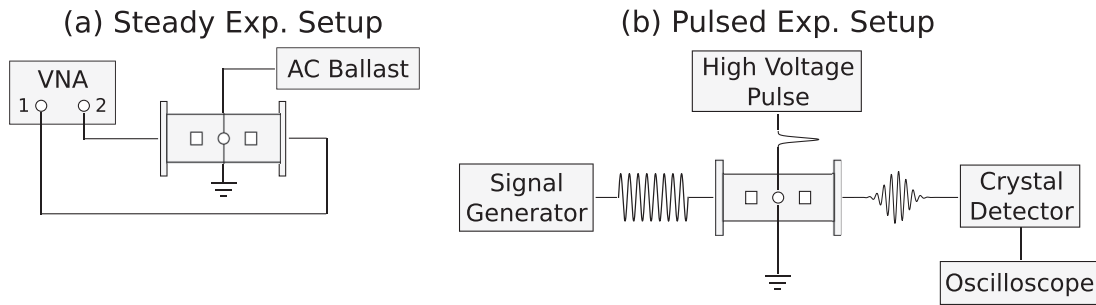


FIG. 1. Schematic of the experimental setup used to measure the plasma-resonator microwave response with a steady state plasma (a) and pulsed plasma (b).

plasma is assumed to fill the quartz envelope uniformly to a radius equal to  $\sqrt{2}$  times the inner radius of the tube. This assumption accounts for the fact that wall-loss driven diffusion of the plasma is expected to produce a nearly parabolic density profile, which we do not model. Instead, we take the peak density of the non-uniform profile and spread it uniformly over a smaller radius to generate the same average plasma density.<sup>16</sup>

The cavity consists of two rectangular posts spaced 13.7 mm apart with dimensions 4.4 mm along the wide waveguide axis and 3.94 mm along the propagation direction. The primary cavity resonant mode is a TE<sub>01</sub> mode at 13.73 GHz and 12.275 GHz with and without a cylindrical quartz envelope to confine a plasma discharge. The quality factor similarly decreases from 2500 to 2100 with the quartz envelope. The second resonance is calculated to be a TE<sub>02</sub> mode at 21 GHz, which is sufficiently outside of the typical WR-62 band of 12–18 GHz, and so simulations assume the presence of a single cavity mode.

The device is fabricated using additive manufacturing with plastics to form a scaffold onto which a 10  $\mu\text{m}$  coating of copper is electroplated to create conducting surfaces. A hole is centered above the resonant cavity in order to insert a cold fluorescent lamp (CFL) and introduce a plasma into the cavity. The CFL has a 4 mm outer diameter with a wall thickness of 1 mm and is filled to approximately 5 Torr with argon and mercury. The plasma resonator system is first characterized with a vector network analyzer (HP 8722D), and the CFL is driven by a 70 kHz AC ballast. At this frequency, the plasma density seems to be quasi-steady.<sup>16</sup> Measured RMS voltages range from 105 to 125 V and RMS currents from 0.4 to 2 mA. A schematic of the experimental setup for quasi-steady plasma conditions is shown in Fig. 1(a).

The unsteady response of the cavity is measured by using a high voltage pulse to drive the plasma. The high voltage pulse has a ramp shape that is measured to peak at 4 kV with a width of 260 ns. The voltage drops precipitously as the current pulse ramps up to a peak of 4 A with a width of 55 ns. A signal generator (HP 83732A) outputs a continuous microwave signal between 12 and 18 GHz, typically set to a power of +20 dBm. A microwave crystal detector (Krytar 303S Zero Bias Schottky Detector) positioned downstream of the waveguide resonator measures the transmitted power and data are acquired on a digital oscilloscope. The pulsed experimental setup is shown in the schematic in Fig. 1(b).

The plasma-cavity system is first characterized in a steady state mode with the low frequency plasma discharge.

The simulation results are used as a mapping between the measured resonance frequency shift and inferred plasma density. In the experiment, the current supplied to the CFL is increased to shift the resonant frequency to higher values. In both the simulation and experiment, the quality factor and peak transmittance of the plasma-cavity system decrease with increasing plasma density. The simulation and experimental results using the AC discharge are shown in Fig. 2. It is noteworthy that there is an additional small peak in the experimental data seen at the unfilled cavity resonance frequency that is not reproduced in the simulation. The instrumental uncertainty in the frequency shift was measured to be  $\pm 0.73$  MHz, which corresponds to an uncertainty in the plasma density of  $\pm 1.66 \times 10^{10} \text{ cm}^{-3}$ . We compared our measured plasma density with the zero-dimensional discharge model also described by Wang and Cappelli<sup>16</sup> and found the electron densities to be within 65% of that expected from the model. The differences suggest that confidence in the plasma densities is likely to be within a factor of two of those reported in our figures.

The pulsed response of the plasma-cavity system is studied by driving the plasma with a high voltage pulse. Both the growth and decay of the plasma density change the resonant frequency of the cavity from the initial frequency, up to a maximum frequency, and back down to the initial frequency. A CW input microwave signal with a frequency set to 12.275 GHz, the zero-plasma resonance frequency, will be

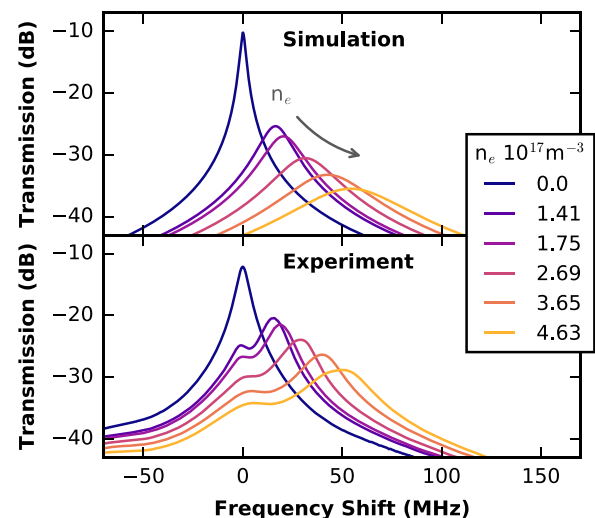


FIG. 2. Simulated (top) and experimentally measured (bottom) frequency responses of the resonant cavity with various plasma densities partially filling the cavity.

reflected for the duration of the plasma, around 0.6 ms. If the CW input signal is then increased to higher frequencies, the resonance condition corresponds to a non-zero plasma density. Only when this condition is met will the microwaves couple through the cavity and transmit to the receiver. The time response of the plasma directly results in a pulsed response of the microwave signal, which can be shaped by selecting the input signal frequency. Microwave pulse responses from input frequencies of 12.275 to 13.275 GHz are shown in Fig. 3(a). In this figure, the transmission power is normalized by the insertion loss of the cavity, and only microwave pulses on the decaying slope of the plasma density are shown.

The variation in pulse delay time and pulse width with input frequencies ranging from 12.275 to 15.275 GHz is shown in Fig. 3(b). Again the characteristics presented in this figure are for those pulses generated on the decaying slope of the plasma density. The delay time of the microwave pulse, defined here as the time between the rising slope of the current pulse and the microwave pulse, decreases monotonically with increased input frequency from 0.6 ms to 29  $\mu$ s. This is due to the monotonic decay of plasma density, with higher plasma densities corresponding to higher resonance frequencies. On the other hand, the pulse width depends both on the decay rate of the plasma and the quality factor of the cavity. The former increases exponentially in

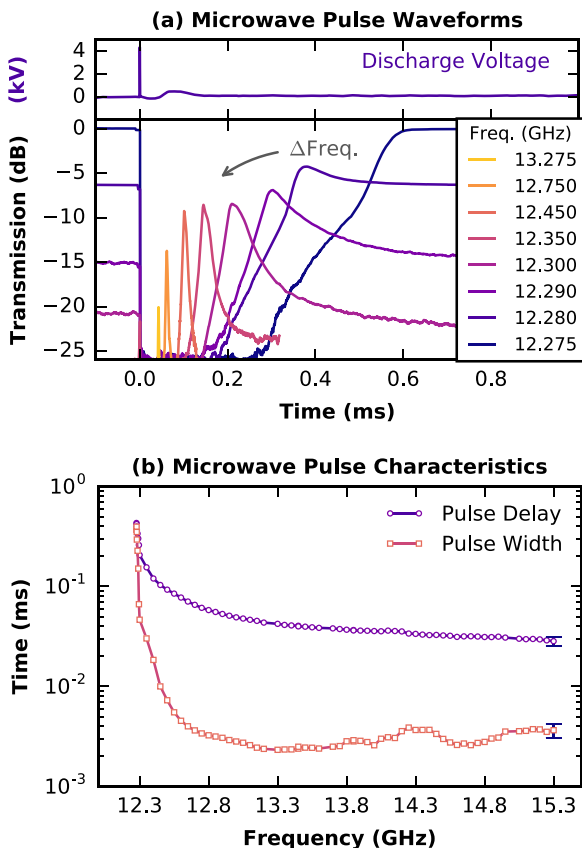


FIG. 3. A pulsed plasma discharge and its time varying electron density correspondingly create a time varying frequency response in the plasma-cavity system. Transmitting a CW input signal results in an output of a microwave pulse that may be shaped by varying the input frequency. Waveforms of pulses for various input frequencies shown in (a) and pulse characteristics of delay and width shown in (b).

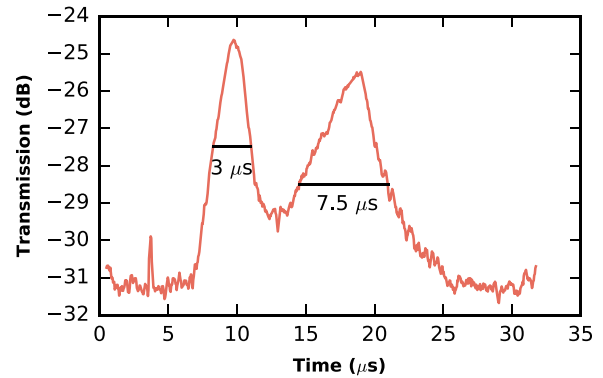


FIG. 4. Microwave double pulse formed with the plasma-cavity system from the rising and decaying slopes of the plasma density with a pulsed discharge.

frequency, while the latter decreases exponentially in frequency. This can be seen as the pulse width rapidly decreases to 2.5  $\mu$ s with increasing frequency from 12.3 to 13.3 GHz, but from 13.3 to 15.3 GHz, the width found to slightly increase. In this way, the pulse characteristics may be shaped by setting the input microwave frequency. The drawback is that for narrow pulse widths, the transmission is reduced significantly. The measured instrumental uncertainty here was  $\pm 3 \mu$ s for the pulse delay and  $\pm 0.6 \mu$ s for the pulse width.

Thus far, we have presented microwave pulses produced from the decaying slope of the plasma density, but microwave pulses are formed on the rising slope as well. These pulses are more difficult to detect due to noise from the high voltage pulse circuit. An example of a double pulse detected at an input microwave frequency of 17.3 GHz is shown in Fig. 4. The first pulse is seen to be more narrow with a width of 3  $\mu$ s when compared to the second pulse which has a measured width of 7.5  $\mu$ s. The difference in pulse width is attributed to the difference in ionization and decay timescales.

The variation in plasma density with time may be reconstructed from the microwave pulse delay measurements of Fig. 3, and the calibrated plasma densities from the steady-state measurements of Fig. 2. The corresponding plot of plasma density variation with time is shown as the circular symbols in Fig. 5. Each measurement of plasma density in

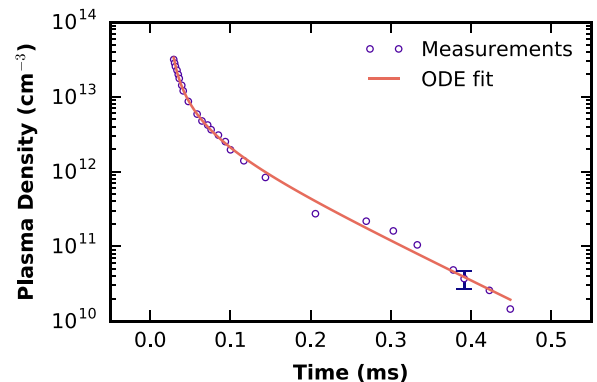


FIG. 5. Time history of the plasma density measured by accruing multiple plasma pulses and increasing the input microwave frequency. Microwave plasma density measurements are shown in circles and a numerical fit of the parameters in the ODE  $dn_e/dt = -\alpha n_e^2 - n_e/\tau$  are shown as a line.

time corresponds to a single plasma pulse. The recombination coefficient ( $\alpha$ ) and characteristic time associated with diffusion ( $\tau$ ) are estimated by numerically fitting the ordinary differential equation for plasma density,  $dn_e/dt = -\alpha n_e^2 - n_e/\tau$ , and are found to be  $\alpha = 3.63 \times 10^{-9} \text{ cm}^3/\text{s}$  and  $\tau = 83.0 \mu\text{s}$ . The recombination time agrees with what was previously reported<sup>10</sup> for discharges in mixtures of argon and mercury. As described, by Sergeichev *et al.*,<sup>10</sup> the recombination time is much longer than a pure argon discharge due to latent ionization of mercury from excited metastable argon atoms. This was an unexpected result to us and leads to the recommendation that for high bandwidth applications, devices relying on the plasma recombination should employ pure argon discharges rather than those containing argon and mercury gas.

In summary, we have presented a microwave resonant cavity that with the addition of a plasma element has a tunable bandpass filter response. The plasma may then be pulsed in order to generate microwave pulses. By controlling the input microwave frequency, the output pulse delay and width may be shaped from hundreds of microseconds to a few microseconds. This technique also allows for the plasma density time history to be reconstructed, which is sensitive over several orders of magnitude in plasma density. Future work includes varying the plasma discharge properties such as fill pressure and higher fidelity simulations that include fluid behavior of the plasma coupled with an electromagnetic solver to study nonlinear effects.

This work was supported by the Air Force Office of Scientific Research (AFOSR) under Award No. FA9550-14-10317 through a Multi-University Research Initiative (MURI) grant titled “Plasma-Based Reconfigurable Photonic Crystals and Metamaterials” with Dr. Mitat Birkan as the program manager.

<sup>1</sup>D. J. Rose and S. C. Brown, *J. Appl. Phys.* **23**, 1028 (1952).

<sup>2</sup>A. W. Trivelpiece and R. W. Gould, *J. Appl. Phys.* **30**, 1784 (1959).

<sup>3</sup>F. W. Crawford, G. S. Kino, S. A. Self, and J. Spalter, *J. Appl. Phys.* **34**, 2186 (1963).

<sup>4</sup>B. Agdur and B. Enander, *J. Appl. Phys.* **33**, 575 (1962).

<sup>5</sup>K. B. Persson, *Phys. Rev.* **106**, 191 (1957).

<sup>6</sup>S. J. Buchsbaum, L. Mower, and S. C. Brown, *Phys. Fluids* **3**, 806 (1960).

<sup>7</sup>J. M. Anderson, *Rev. Sci. Instrum.* **32**, 975 (1961).

<sup>8</sup>M. A. Biondi and S. C. Brown, *Phys. Rev.* **76**, 1697 (1949).

<sup>9</sup>Y.-J. Shiu and M. A. Biondi, *Phys. Rev. A* **17**, 868 (1978).

<sup>10</sup>K. F. Sergeichev, N. A. Lukina, and A. A. Fesenko, *Plasma Phys. Rep.* **39**, 144 (2013).

<sup>11</sup>J. Foster, G. Edmiston, M. Thomas, and A. Neuber, *Rev. Sci. Instrum.* **79**, 114701 (2008).

<sup>12</sup>A. L. Vikharev, A. M. Gorbachev, O. A. Ivanov, V. A. Isaev, S. V. Kuzikov, M. A. Lobaev, J. L. Hirshfield, S. H. Gold, and A. K. Kinkead, *Phys. Rev. Spec. Top.-Accel. Beams* **12**, 062003 (2009).

<sup>13</sup>O. A. Ivanov, V. A. Isaev, M. A. Lobaev, A. L. Vikharev, and J. L. Hirshfield, *Appl. Phys. Lett.* **97**, 031501 (2010).

<sup>14</sup>A. Semnani, A. Venkatraman, A. A. Alexeenko, and D. Peroulis, *Appl. Phys. Lett.* **103**, 063102 (2013).

<sup>15</sup>A. Semnani, K. Chen, and D. Peroulis, *IEEE Microwave Wireless Compon. Lett.* **24**, 351 (2014).

<sup>16</sup>B. Wang and M. A. Cappelli, *Appl. Phys. Lett.* **107**, 1 (2015).